Accumulation capacitance of narrow band gap metal-oxide-semiconductor capacitors

Erik Lind,[1,a)] Yann-Michel Niquet,[2] Hector Mera,[2] and Lars-Erik Wernersson[1,3]
[1]*Solid State Physics, Lund University, Box 118, 22100 Lund, Sweden*
[2]*CEA-UJF, INAC, SP2M/L_Sim , 17 rue des Martyrs, 38054 Grenoble Cedex 9, France*
[3]*Electrical and Information Technology, Lund University, Box 118, 22100 Lund, Sweden*

(Received 30 April 2010; accepted 18 May 2010; published online 9 June 2010)

We have investigated the accumulation capacitance-voltage characteristics for capacitors with narrow band gap materials using modeling and experiments. The capacitance for InAs and $In_{0.53}Ga_{0.47}As$ capacitors with a HfO_2 oxide layer has been calculated using atomistic tight-binding, effective mass, and semiclassical nonparabolic models. The simulations show that band structure effects have a strong influence on the accumulation capacitance, and are essential for the description of narrow band gap capacitors. The calculated tight binding data compare well with measurements on n-type InAs HfO_2 capacitors on (100) and (111)B substrates, highlighting the nonparabolicity as the main origin for the large accumulation capacitance. © *2010 American Institute of Physics*. [doi:10.1063/1.3449559]

The performance of metal-oxide-semiconductor (MOS) field-effect-transistors can potentially be enhanced by using narrow band gap III–V semiconductors as the channel material.[1–3] In this context, capacitance-voltage (CV) measurements on MOS capacitors (MOSCAPs) are an important tool used to characterize the physical properties and quality of the III–V semiconductor interface.[4] The CV data are usually interpreted through comparisons with simulations based on the effective mass approximation. There is currently a strong interest in MOS field-effect-transistors and MOSCAPs based on narrow band gap materials, such as InAs (Refs. 5 and 6) and $In_xGa_{1-x}As$ $(x>0.5)$.[7,8] However, the interpretation of CV data is not straightforward in narrow band gap MOSCAPs with thin, high-κ oxides. This is mainly due to quantum confinement, and to the strong nonparabolicity of the conduction band.[9] Indeed, the conduction band effective mass tends to be small in narrow band gap materials, which leads to small density of states and semiconductor capacitances. For a MOSCAP biased in the strong accumulation regime, the Fermi level can therefore rise high above the conduction band edge. Thus, nonparabolicity effects must be taken into account to avoid large errors in the calculated capacitances, which can make data interpretation difficult. The small conduction band effective mass can further lead to strong quantum quantization, especially in the accumulation region, where the charge carriers are confined at the semiconductor-oxide interface.

In this letter, we compare experimental CV data from n-type InAs high-κ MOSCAPs, with capacitance calculations using a $sp^3d^5s^*$ tight binding (TB) model, a semiclassical nonparabolic model (SCNP),[9] an effective mass Schrödinger–Poisson solver (EM), and a semiclassical effective mass approximation (SCEM). It is clearly shown that the effective mass models underestimate the semiconductor accumulation capacitance with respect to the TB and SCNP calculations. Quantum effects are shown to be substantially smaller in the accumulation region than nonparabolicity effects. The TB model shows very good agreement with our measured data from InAs MOSCAPs with various substrate orientations and oxide thicknesses.

MOSCAPs were fabricated on (100) and (111)B InAs wafers with nominal n-type doping $N_d=3.0\times10^{16}$ cm^{-3} and $N_d=7.0\times10^{16}$ cm^{-3}, respectively. The samples were etched for 1 min using $HCl:H_2O$ (1:1) and rinsed in 2-isopropanole for 20 s, then loaded into a Cambridge Nanotech Savannah-100 atomic layer deposition system. 2.5 and 6-nm-thick HfO_2 films were grown using 35 cycles and 80 cycles, respectively, of tetrakis(dimethylamido)hafnium and H_2O, at a deposition temperature of 250 °C. The relative dielectric constant of the deposited HfO_2 is 21 ± 2, as obtained from measurements of reference HfO_2 diodes on n-type Si. The HfO_2 thickness was calibrated through reference thickness series depositions on Si, and subsequent thickness determination using a variable angle spectroscopic ellipsometer. This leads to nominal oxide capacitances $C_{ox}=31\pm3$ $fF/\mu m^2$ for the 6 nm samples and $C_{ox}=81\pm7$ $fF/\mu m^2$ for the 2.5 nm sample. W/Au contacts with areas of 2560 μm^2 were formed using dc sputter deposition, optical contact lithography, and etching. CV data was then obtained at an oscillation amplitude of $v_{ac}=30$ mV, at frequencies between $f=100$ kHz and 35 MHz, using an Agilent 4294A impedance analyzer and a Cascade 11000B shielded probe station. The measurement temperature was $T=220$ K.

The TB capacitances were computed with a fully atomistic Schrödinger–Poisson solver based on the $sp^3d^5s^*$ TB model of Ref. 10. The density of conduction band electrons is calculated from the band structure and wave functions of a 250-nm-thick semiconductor film sampled over 2400 transverse **k** points around Γ. By solving Poisson's equation self-consistently, the total semiconductor charge, Q_s, and the semiconductor capacitance, $C_s\propto dQ_s/d\phi_s$, can be calculated as a function of the surface potential, ϕ_s. In the accumulation regime, and in the absence of border traps, C_s corresponds to the high-frequency capacitance. For the EM calculations, we also used a self-consistent Schrödinger–Poisson solver, based on the effective mass approximation instead of the tight-binding method. Both the TB and EM approaches describe quantum confinement but only the former reproduces the

a)Electronic mail: erik.lind@ftf.lth.se.

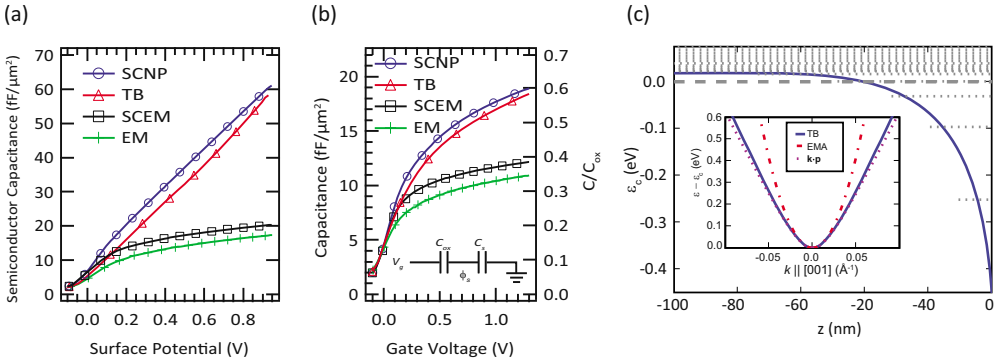

FIG. 1. (Color online) (a) Calculated InAs semiconductor capacitance C_s vs surface potential ϕ_s, using the SCNP, TB, SCEM, and EM models ($N_d=3.0\times10^{16}$ cm^{-3} and $T=220$ K). (b) Calculated InAs CV–data with $C_{ox}=31.6$ fF/μm^2 and $N_d=3\times10^{16}$ cm^{-3}. The inset shows the relation between C_{ox}, C_s, and total gate capacitance C_g. (c) Conduction band profile from the TB model, at a gate bias $V=1$ V. The Fermi level (dashed line) is taken as the reference energy. The dotted lines are the subband edges. The inset shows the bulk conduction band structure of InAs in the TB, effective mass (EMA), and two-band $\mathbf{k}\cdot\mathbf{p}$ approximations.

nonparabolicity of the conduction band. For the semiclassical SCNP calculations, we followed Ref. 9, which is based on a two-band $\mathbf{k}\cdot\mathbf{p}$ model. The carrier density in the conduction band is here given by Eq. (1),

$$n(\phi)=\frac{2N_c}{\sqrt{\pi}}\int_0^\infty \frac{\sqrt{\varepsilon(1+\alpha\varepsilon)}(1+2\alpha\varepsilon)d\varepsilon}{1+\exp(\varepsilon-\phi)}. \quad (1)$$

Here, $\varepsilon=(E-E_c)/kT$ is the normalized electron kinetic energy, $\phi=(E_f-E_c)/kT$ is the normalized Fermi energy, and N_c is the effective conduction band density of states. The nonparabolicity factor, $\alpha=(1-m_e/m_0)^2/\varepsilon_g$, is enhanced by a small effective mass m_e and a narrow normalized gap $\varepsilon_g=(E_c-E_v)/kT$. For $\alpha=0$, this model reduces to the traditional SCEM with Fermi–Dirac statistics. Neither the SCNP nor the SCEM approach takes quantum confinement into account. We therefore expect the TB model to provide the most accurate results, since it reproduces the full band structure and describes quantum confinement effects.

Figure 1(a) shows the semiconductor capacitances C_s for an InAs MOSCAP, calculated using the TB, EM, SCNP, and SCEM approaches. The doping is $N_d=3.0\times10^{16}$ cm^{-3} and the temperature is $T=220$ K. For the SCNP, SCEM, and EM calculations, the parameters are $m_e=0.023$ m_o and $E_g=0.36$ eV. A surface potential of $\phi_s=0$ corresponds to flatband condition. We note a striking difference between the parabolic and nonparabolic models. The semiconductor capacitance increases slowly for ϕ_s in the effective mass approximation (SCEM and EM), while it increases almost linearly in the nonparabolic SCNP and TB approaches, due to the faster increase in the density of states with energy for those models. While nonparabolicity increases C_s, quantum confinement reduces the density of states and moves the charge centroid away from the semiconductor-oxide interface. This decreases the semiconductor capacitance, as can be seen by comparing the TB and SCNP, and EM and SCEM models, respectively, in Fig. 1(a). The reduction in C_s due to quantum confinement is, however, substantially weaker than the increase due to nonparabolicity, especially for large ϕ_s. Thus, nonparabolicity effects must be primarily included for accurate calculations of the capacitance in narrow band gap materials.

Figure 1(b) shows the CV data calculated with the different models, for $C_{ox}=31.6$ fF/μm^2. Since $C_g=C_{ox}/(1+C_{ox}/C_s)$, the differences between the calculated C_g are smaller than those between C_s. Nevertheless, at $V_g=1$ V the SCEM and EM model underestimate the capacitance by about 50% with respect to the TB model. The SCNP and TB models, which both account for nonparabolicity, are on the other hand in fairly good agreement in the accumulation region.

Figure 1(c) shows the calculated conduction band profile from the TB model at $V_g=1.0$ V. Due to the thin oxide thicknesses (<6 nm) and large gate bias (1 V), the Fermi level reaches up to about 0.6 eV above the conduction band edge, where band structure effects are significant. This is clearly evidenced in the inset of Fig. 1(c). At this bias, we also observe that only four subbands are occupied below E_f. In spite of quantum confinement, the nonparabolic behavior of the conduction band leads to large C_s and C_g. We have also performed calculations for an $In_{0.53}Ga_{0.47}As$ MOSCAP,[7,8] as shown in Fig. 2. Since the effective mass and band gap of $In_{0.53}Ga_{0.47}As$ ($m^*=0.041$ m_0 and $E_g=0.76$ eV) are larger than those of InAs, the discrepancies between the SCEM/EM and TB/SCNP models are smaller. Nevertheless, the SCEM model gives capacitances 20% smaller than the TB model at $V_g=1$ V. Thus, for an accurate fit of the accumulation capacitance, the inclusion of band structure effects is important also in $In_{0.53}Ga_{0.47}As$ MOSCAPs.[7,8]

Some extraction techniques for the density of interface traps (D_{it}), such as the low-frequency and Terman methods[4,7]

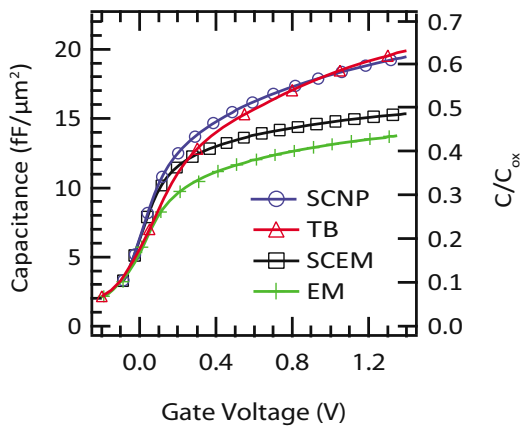

FIG. 2. (Color online) Calculated capacitance for an $In_{0.53}Ga_{0.47}As$ capacitor with $C_{ox}=31.6$ fF/μm^2 and $N_d=7.2\times10^{16}$ cm^{-3}.

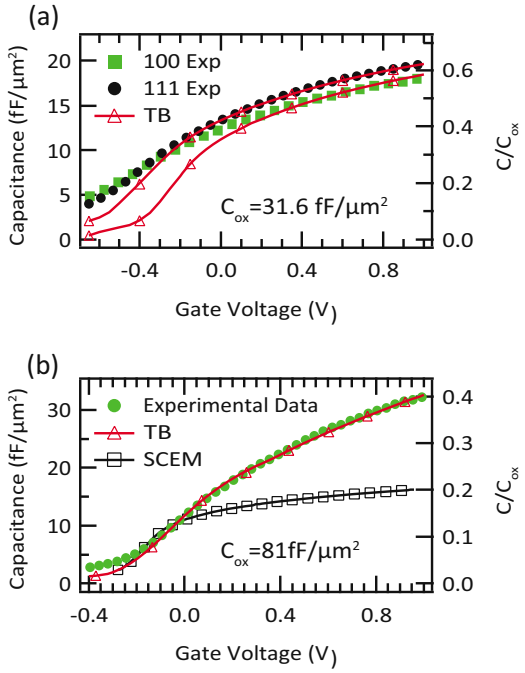

FIG. 3. (Color online) (a) Comparison between experimental and TB data for InAs (100) and (111) MOSCAPs with $t_{ox}=6$ nm and $C_{ox}=31.2$ fF/μm^2. (b) Experimental and TB/SCEM data for InAs (100) MOSCAP with $t_{ox}=2.5$ nm, $C_{ox}=81$ fF/μm^2, and $N_d=3\times10^{16}$ cm^{-3}.

rely on a comparison between calculated and measured capacitance data. Hence, the effective mass approximation can lead to large errors on D_{it} in the accumulation region. Also, due to the nonsaturating semiconductor capacitance, the determination of the oxide capacitance, which is needed for D_{it} calculations through the conductance method[4] is also nontrivial. Here, our simulated data further suggest that C_{ox} can be reliably obtained by fitting the accumulation capacitance to the relatively simple two-band model that captures the essential physics.

To verify our findings, we have compared the experimental and simulated capacitances for InAs MOSCAPs. Figure 3(a) shows the measured CV-data ($f_{osc}=10$ MHz) for the (100)- and (111)B-samples with $t_{ox}=6.0$ nm, along with the TB data. Good fits between theory and experiment are obtained in the strong accumulation region, after a flat-band voltage shift $V_T=-0.3$ V for the (100) and $V_T=-0.45$ V for the (111)B samples. For voltages below $V_g-V_T=-0.5$ V, the simulated and experimental curves deviate. We attribute this difference to trap response from interface/border defects, which are not included in our model. Interestingly, D_{it} seems to be smaller in (111)B than in (100) MOSCAPs, as there is a smaller stretch-out in the negative bias region. Frequency dependent (10 kHz–35 MHz) studies show a logarithmic frequency dispersion in the accumulation regime, with a reduction in the capacitance of around 0.8 fF/μm^2 per decade (essentially independent of temperature), which we attribute to border traps[11] in the HfO_2 oxide (data not shown). While the dispersion is not zero at our highest measurement frequency (35 MHz), it is gradually decreasing. The error due to charge traps in the oxide can thus be roughly estimated to 1–2 fF/μm^2, which is substantially less than the band structure effects discussed in this work. Figure 3(b) shows the experimental and simulated (TB/SCEM) CV curves from the sample with a thinner oxide, $t_{ox}=2.5$ nm, obtained at $f_{osc}=30$ MHz. Again, good agreement between the TB and experimental data is achieved, with a V_T shift of -0.18 V. In particular, we note an even stronger increase in the accumulation capacitance, as the larger oxide capacitance enhances the contribution of the semiconductor capacitance, in line with the above discussion.

To conclude, we have experimentally and theoretically investigated the accumulation capacitance of narrow band gap III–V MOSCAPs. It is shown that the introduction of nonparabolic effects is necessary to accurately describe the shape of the CV curve. A reasonable fit can nonetheless be obtained in the strong accumulation regime using a simple two-band semiclassical model, disregarding confinement effects.

This work was supported in part by the Swedish Foundation for Strategic Research (SSF), the Knut and Alice Wallenberg Foundation, by the Swedish Research Council (VR), and the Swedish Governmental Agency for Innovation Systems (VINNOVA). Parts of the calculations were run at the French CCRT.

[1]U. Singisetti, M. A. Wistey, G. J. Burek, A. K. Baraskar, B. J. Thibeault, A. C. Gossard, M. J. W. Rodwell, S. Byungha, E. J. Kim, P. C. McIntyre, Y. Bo, Y. Yu, D. Wang, T. Yuan, P. Asbeck, and Y.-J. Lee, IEEE Electron Device Lett. **30**, 1128 (2009).
[2]Y. Xuan, Y. Q. Wu, and P. D. Ye, IEEE Electron Device Lett. **29**, 294 (2008).
[3]M. Egard, S. Johansson, A. C. Johansson, K. M. Persson, A. W. Dey, B. M. Borg, C. Thelander, L. E. Wernersson, and E. Lind, Nano Lett. **10**, 809 (2010).
[4]E. H. Nicolian and J. R. Brews, *MOS (Metal Oxide Semiconductor) Physics and Technology* (Wiley, New York, 1981).
[5]N. Li, E. S. Harmon, J. Hyland, D. B. Salzman, T. P. Ma, Y. Xuan, and P. D. Ye, Appl. Phys. Lett. **92**, 143507 (2008).
[6]D. Wheeler, L. E. Wernersson, L. Fröberg, C. Thelander, A. Mikkelsen, K. J. Weststrate, A. Sonnet, E. M. Vogel, and A. Seabaugh, Microelectron. Eng. **86**, 1561 (2009).
[7]G. Brammertz, H. C. Lin, M. Caymax, M. Meuris, M. Heyns, and M. Passlack, Appl. Phys. Lett. **95**, 202109 (2009).
[8]Y. Hwang, R. Engel-Herbert, N. G. Rudawski, and S. Stemmer, Appl. Phys. Lett. **96**, 102910 (2010).
[9]V. Ariel-Altschul, E. Finkman, and G. Bahir, IEEE Trans. Electron Devices **39**, 1312 (1992).
[10]J.-M. Jancu, R. Scholz, F. Beltram, and F. Bassani, Phys. Rev. B **57**, 6493 (1998).
[11]F. P. Heiman and G. Warfield, IEEE Trans. Electron Devices **12**, 167 (1965).